



The Evolution of Post-SM4 Bias Striping Noise in the ACS/WFC

M. C. McDonald, N. A. Grogin

August 2, 2024

ABSTRACT

After the Hubble Space Telescope’s Servicing Mission 4 (SM4) replaced electronics in the Advanced Camera for Surveys (ACS), images taken with the Wide Field Channel (WFC) detector presented a new feature: low-level, horizontal striping caused by $1/f$ noise from the replacement electronics. This “bias striping” effect is uniform across CCD rows and can be effectively removed using the `acs_destripe` tool in `calacs`. In this work, we use raw bias frames from 2009 through 2023 to measure the row-dependent striping noise intensity in an effort to investigate how bias striping noise has evolved over time. We utilize summary statistics such as variance, skewness, and kurtosis, as well as outlier measurements, to better understand the characteristics of the striping noise distributions, ultimately confirming that bias striping noise has remained relatively stable since its initial detection post-SM4.

1 Introduction

The Side-2 electronics failure in January 2007 resulted in the loss of the Advanced Camera for Surveys Wide Field Channel (ACS/WFC) functionality, until the ACS CCD Electronics Box (CEB) and Low Voltage Power Supply (LVPS) were replaced via Servicing Mission 4 (SM4). These replacement electronics, particularly the SIDECAR Application-Specific Integrated Circuit included with the CEB, introduced low frequency noise (1mHz to 1Hz) on the bias and reference voltages it generates for the WFC CCDs (Grogin et al., 2011). A portion of this noise manifests in post-SM4 WFC images as horizontal “bias stripes,”

that vary in intensity, but are uniform with respect to row across each CCD chip. Because the bias striping is highly consistent across all four amplifier readouts, the striping noise in WFC1 is virtually identical to the striping noise in a Y-inverted WFC2.

Bias striping noise was previously characterized in Grogin et al. (2011), where bias frames organized by anneal period were used to assess the stability of bias striping during the first year following SM4. Stripe intensities were measured from 319 bias frames taken from July 2009 to June 2010, and the resulting histogram of these data showed that the bias striping amplitude appears to be highly stable with time. Furthermore, the striping mitigation approaches described in Grogin et al. (2011) led to the development of the current bias striping correction algorithm, `acs_destripe`, which is available in `calacs` and is used to effectively remove bias stripes from ACS/WFC post-SM4 data.

2 Data and Analysis

In this report, we continue the work done in Grogin et al. (2011) by extending the bias striping stability analysis from 2009 through 2023, in an effort to characterize how the bias striping noise has evolved over time. For each year, raw bias frames from the ACS CCD Daily Monitor calibration program were gathered and organized by anneal period. The bias reference file, or “superbias,” for each anneal period was also identified. For each raw bias analyzed, the corresponding superbias was subtracted from the raw bias to remove fixed bias structure and reveal the striping noise.

Once the striping noise had been isolated for a given raw file, the commanded gains per amplifier were extracted from the CCDTAB reference file, and a gain conversion with respect to each amplifier was applied to the data. This conversion is necessary to ensure pixels are properly adjusted for an amplifier’s specific readout characteristics. The physical prescans and virtual overscans were also trimmed from the data to ensure only true SCI pixels were being used.

Given the bias striping uniformity across all four amplifiers, we decided to flip the WFC2 data array with respect to the Y-axis, and join a given row’s data with the corresponding row data from WFC1. This stacking of row arrays resulted in each of the 2,048 rows having 8,192 pixel values, encompassing measurements from both WFC1 and WFC2 to increase the SNR. A 3σ clipping was applied on a row-by-row basis, and then the mean of each row was calculated to determine the average bias striping intensity, per row. Once all row means were gathered for a given file, sigma clipping was applied a second time to ensure any remaining outliers were removed from the data.

The sigma-clipped, row averaged bias striping intensity values for a given bias file were zero-meant, shifting the distribution of values so that they centered around zero. Final striping noise measurements per row were recorded for all bias files taken from 2009 through 2023. A gaussian fitter algorithm, utilizing the Levenberg-Marquardt least-squares minimization technique (MPFIT, Koposov et al. (2024)), was then applied to each year’s data to produce histogram statistics of bias striping noise intensity for each year.

We also recorded the number of raw bias files used in this analysis for each year, shown in Table 1. Prior to 2015, the CCD Daily Monitor programs required four bias frames to be executed every Monday, Wednesday and Friday of each week. This specification changed

during the second CCD Daily Monitor program of Cycle 22, proposal 13953 (Golimowski & Ogaz, 2015), where only two bias frames were requested for execution on these days. As a result, the number of bias frames available per year after 2014 reduced by half. The total number of bias files used for 2009 is also lower than following years, due to ACS not returning to science until July of that year, subsequent to SM4.

Table 1: Total number of raw bias exposures used per year

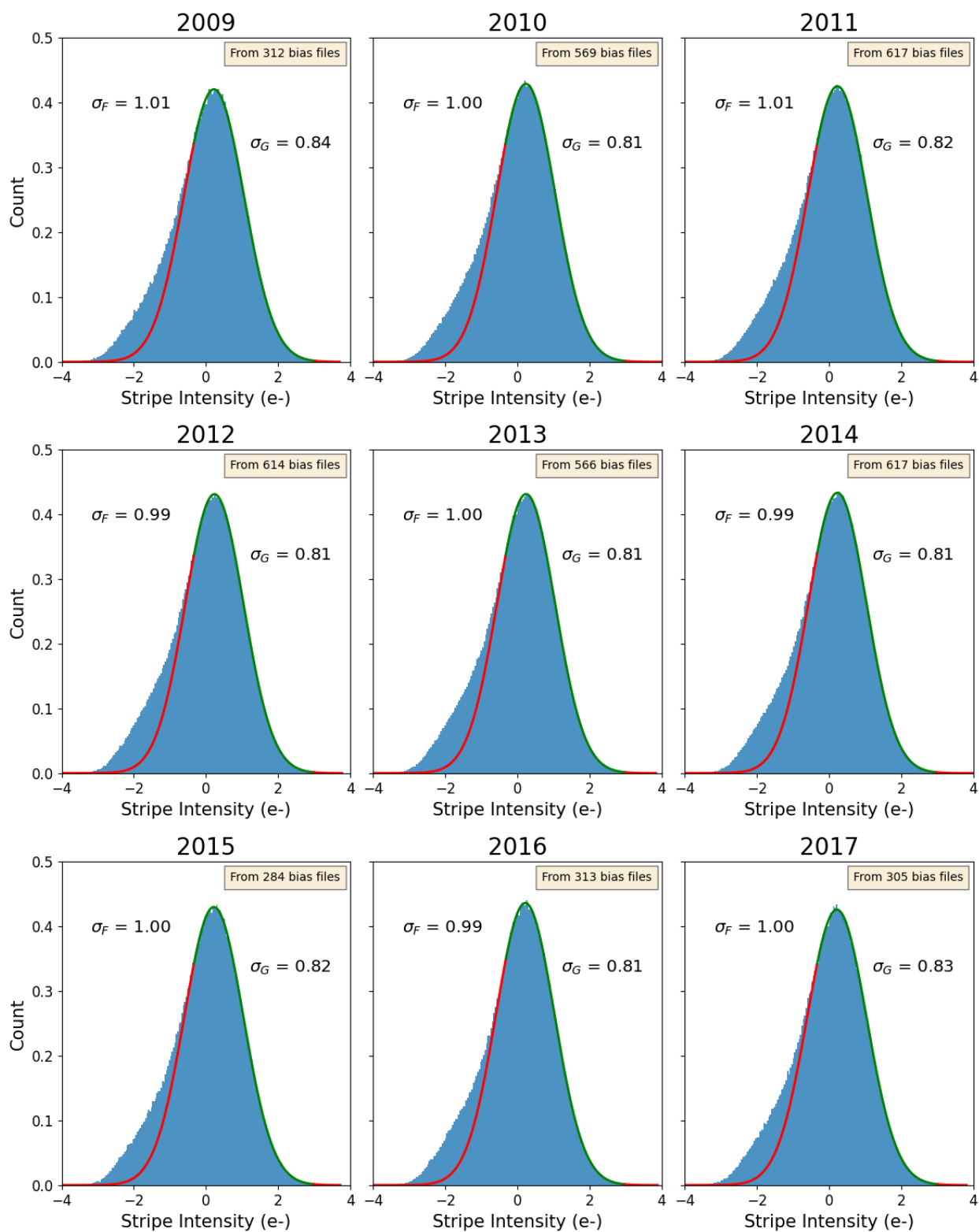
| Year | Number of Bias Exposures |
|-------|--------------------------|
| 2009 | 312 |
| 2010 | 569 |
| 2011 | 617 |
| 2012 | 614 |
| 2013 | 566 |
| 2014 | 617 |
| 2015* | 284 |
| 2016 | 313 |
| 2017 | 305 |
| 2018 | 283 |
| 2019 | 303 |
| 2020 | 305 |
| 2021 | 283 |
| 2022 | 303 |
| 2023 | 247 |

* January 2015 marked the switch to two bias files being taken every Monday, Wednesday, and Friday of each week as part of the CCD Daily Monitor Program. Prior to this, four bias frames were taken on each of these days.

3 Results

The histograms of bias stripe intensities with best-fit Gaussian models for each year are plotted in Figure 1. The standard deviation of the full distribution (σ_F) and the fitted Gaussian (σ_G) are also featured in each plot, along with the number of bias files analyzed for a given year. We observe similar, negatively skewed distributions for each year, made more apparent by the overlaying of the best-fit Gaussian as determined by MPFIT.

To better illustrate how the distributions evolve over time, we synthesize all 15 years of data into a stacked density plot, displayed in Figure 2. The overall distribution of each year’s striping noise appears to remain relatively unchanged with time. To reaffirm this assumption, we use the σ_F and σ_G measurements to create a sigma time-series plot, featured in Figure 3. The long-term stability of both sigma measurements is apparent in this plot, despite years 2019 and 2022 presenting with notably lower σ_F values, $0.94e^-$ and $0.95e^-$, respectively, in comparison to the other years.



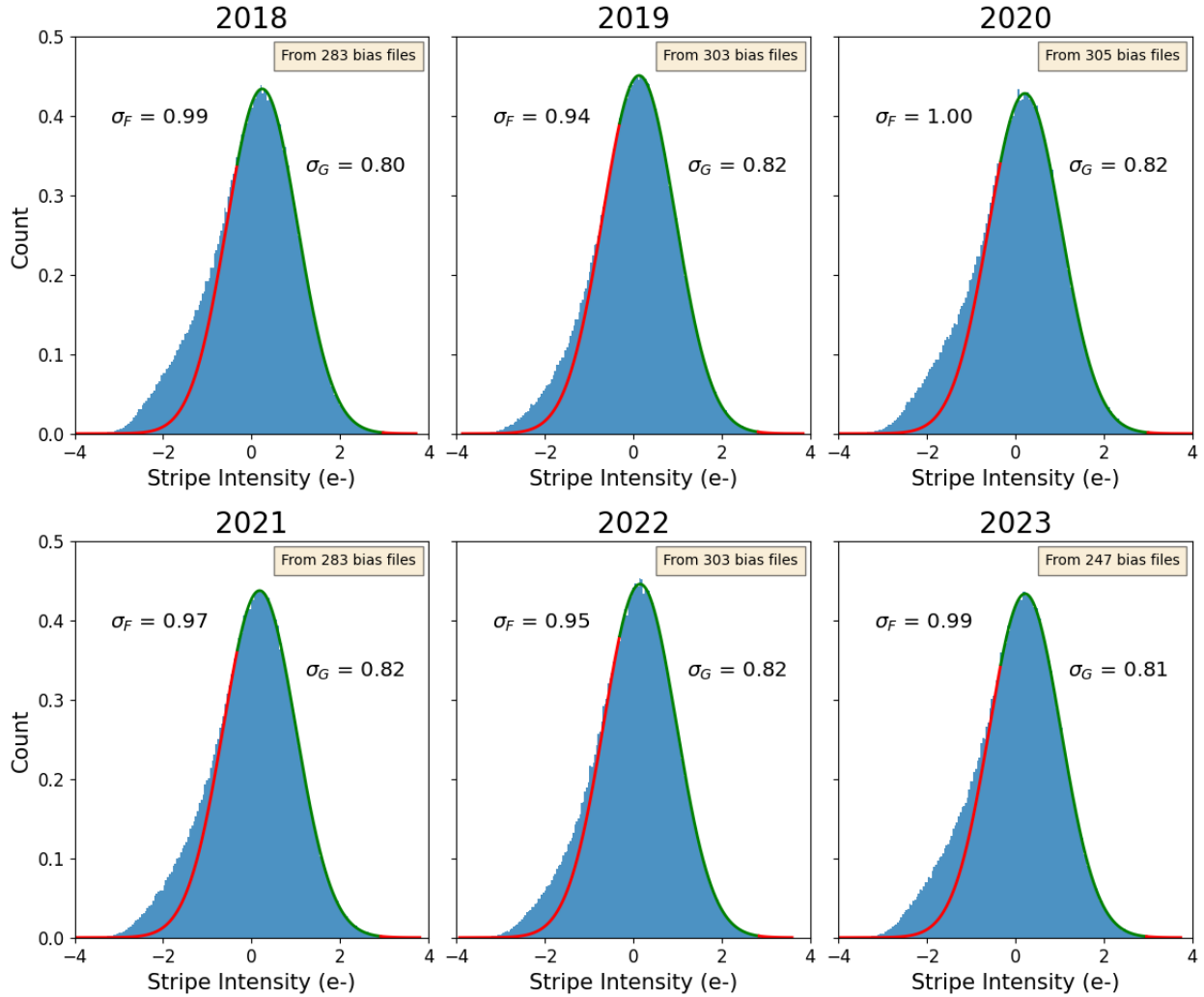


Figure 1: Histograms of ACS/WFC bias striping intensities for years 2009 through 2023. The histogram for the full distribution uses 200 bins and is featured in blue, while the best-fit Gaussian is plotted in green and red, indicating the restricted domain of histogram fitting to the Gaussian model. The standard deviation of the full distribution (σ_F) and Gaussian model (σ_G) are also given for each year, as well as the total number of raw bias files used. All plots share the same X- and Y-axis scaling and range.

In an effort to better understand the characteristics of the striping noise distributions, we calculate both the skewness and kurtosis measurements from each year’s data. Skewness allows us to ascertain the symmetry of a distribution, where zero skewness indicates a normal distribution with balanced tails, positive skewness indicates the presence of a tail on the right, and negative skewness indicates the presence of a tail on the left. Similarly, the kurtosis measurement is used to gauge the “tailedness” of a distribution, which is directly correlated with the number of outliers present. Under the Fisher method, a kurtosis value of zero indicates a normal distribution, a positive kurtosis value indicates a more “peaked” distribution due to an increased number of outliers, and a negative kurtosis value indicates a “flatter” distribution due to very few outliers.

The resulting skewness and kurtosis measurements from each year’s striping noise distri-

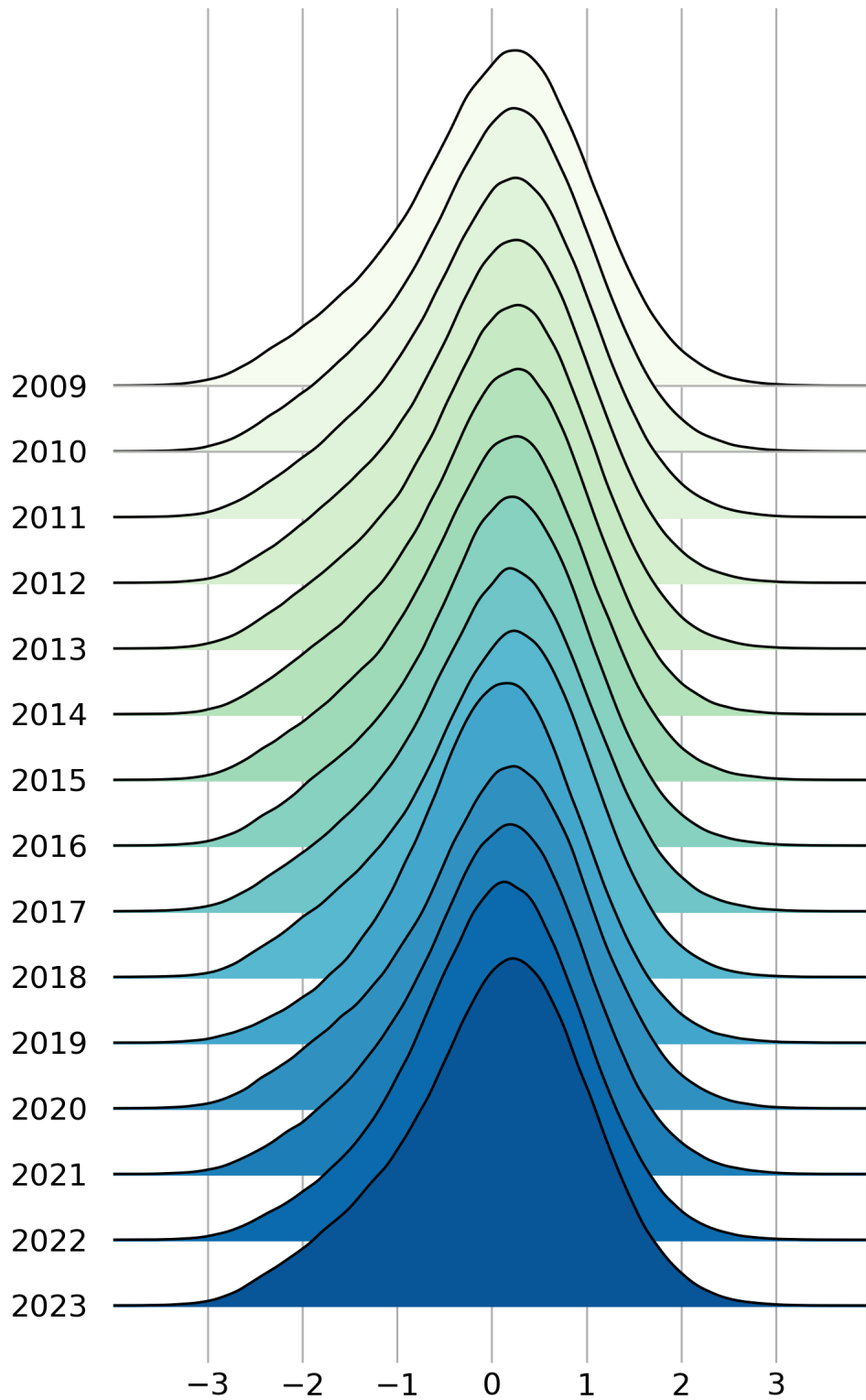


Figure 2: Stacked density plot of the bias striping distributions from 2009 through 2023. With the chronological stacking, the evolution of the bias striping noise can be better visualized, and the similarity in distribution characteristics is made apparent.

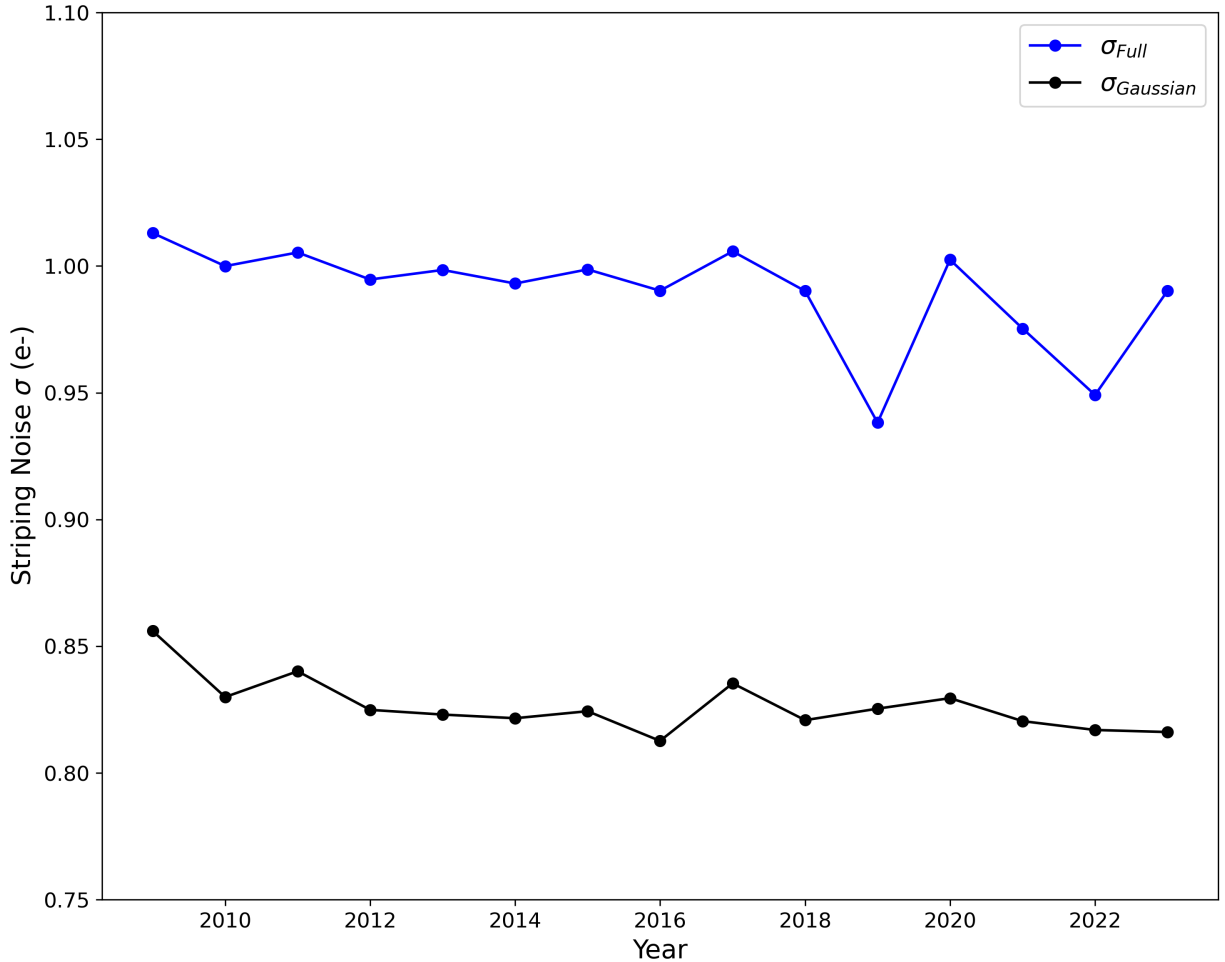


Figure 3: Time series of the full distribution (σ_F) and best-fit Gaussian (σ_G) standard deviation measurements, plotted in blue and black, respectively.

bution are shown in Figure 4. For skewness, all values are negative, confirming that each year’s distribution is slightly negatively skewed and has distinguishable left-sided tails. We see that 2018 data yields the most negative skewness, while 2019, 2021, and 2022 data have the least negative skewness. The differences in skewness measurements are exemplified when comparing the 2018 and 2019 histograms; the histogram for 2018 features a thicker negative tail, while the histogram for 2019 has a noticeably thinner negative tail.

For kurtosis, we observe both positive and negative values, primarily within ± 0.05 of zero, indicating that the distributions are relatively normal (Gaussian) in shape. The majority of kurtosis measurements are slightly negative, while 2019, 2021, and 2022 stand out with positive values. These higher kurtosis values are discernable visually, especially when inspecting the 2019 and 2022 histograms in Figure 1, where the respective distributions appear slightly taller than the years immediately preceding or following.

To determine how skewness and kurtosis may vary for true normal distributions of the same sample size, we perform these calculations on 100 randomly generated Gaussian distributions of sizes 1,200,000 and 600,000 to mimic the approximate number of stripping noise

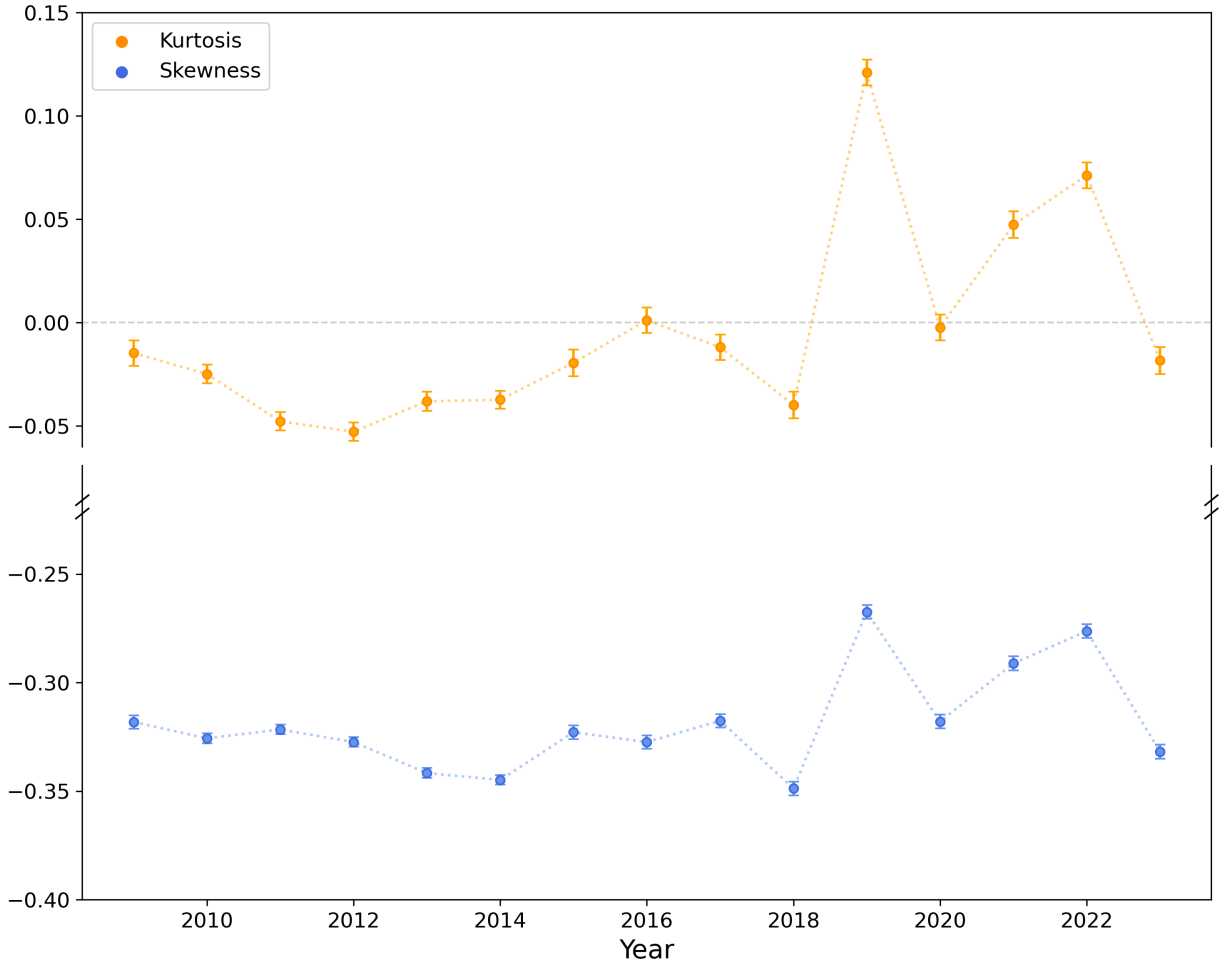


Figure 4: Time series of skewness and kurtosis measurements, plotted in blue and orange, respectively. Each point includes standard error bars that are dependent on sample size, and can be effectively approximated by $6/N$ for skewness and $24/N$ for kurtosis, where N is the total number of bias stripe measurements used for a given year. There is a Y-axis break between -0.05 and -0.25 to allow both metrics to be plotted in the same figure, and for better visualization of the relationship between the two.

values in a given year’s sample, from before and after 2015, respectively. The results are plotted in Figure 5, where we observe scatter around zero within ± 0.01 for skewness and ± 0.02 for kurtosis. These findings are primarily consistent with the scatter seen in the kurtosis and skewness measurements for all years except those with observed deviations: 2019, 2021, and 2022.

To further investigate the deviations found in the sigma, skewness, and kurtosis measurements for 2019, 2021, and 2022, we investigate the number of 3σ and 4σ outliers in each year’s striping noise data to determine if a subset of outliers could be influencing the distributions. Because the number of bias files used for a given year drastically reduces in 2015, we calculate the percent of outliers in a given year’s sample (Figure 6). While the number of 4σ outliers is low and relatively random with time, there is an evident increase in 3σ outliers in 2019, 2021, and 2022, which are the only years where 3σ outliers represent

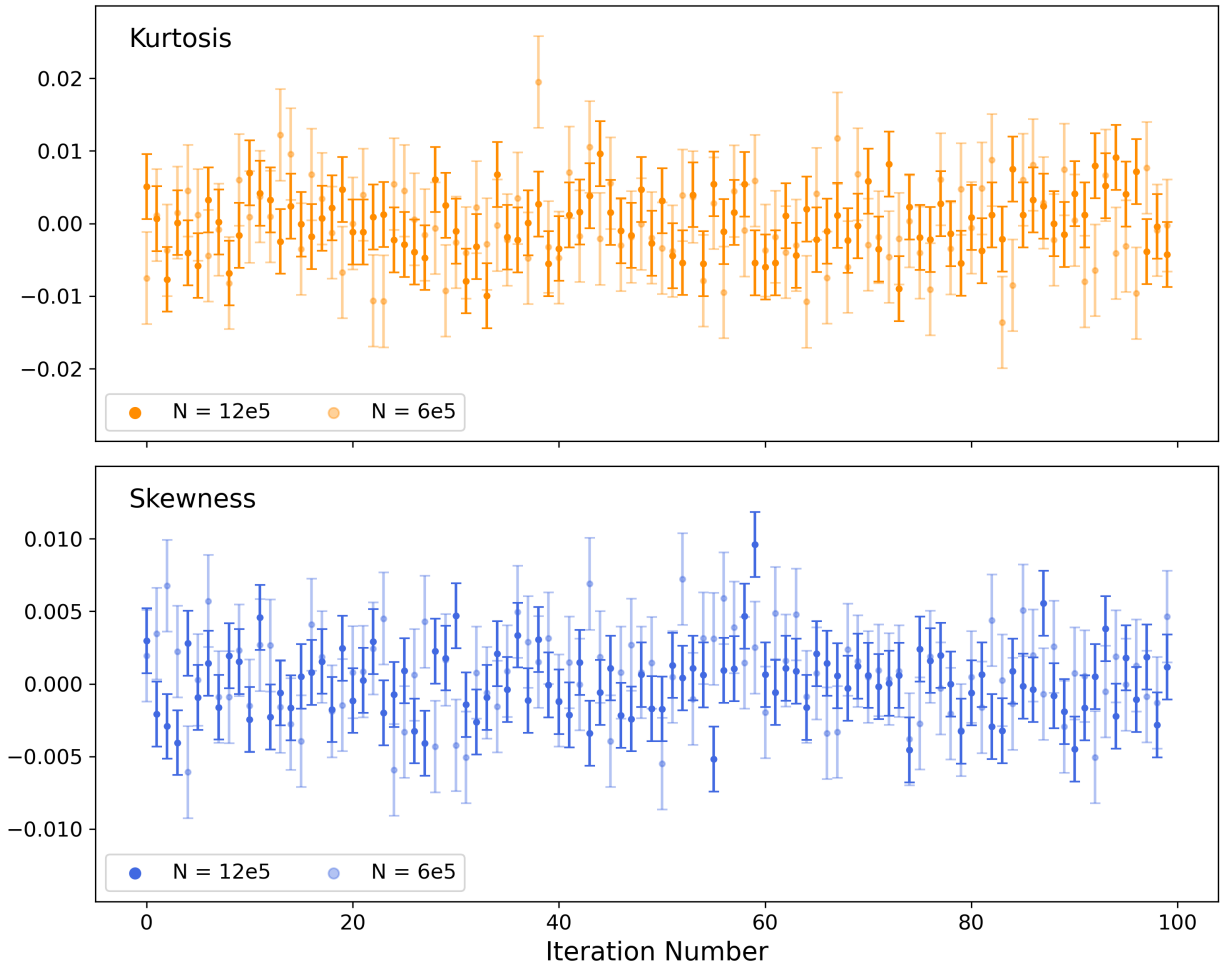


Figure 5: Skewness and kurtosis measurements for 100 randomly generated Gaussian distributions of sample sizes 1,200,000 and 600,000, which mirror the approximate number of bias stripe measurements pre- and post-2015. Blue points correspond to skewness and orange points to kurtosis, with the darker of each shade representing measurements from the larger sample size. Error bars are generated using the same methods as described in Figure 4.

over 0.2% of the sample.

4 Discussion

Upon inspection of how the bias striping intensity distribution evolves over time, we observe no significant change in the 15-year period analyzed, indicating that striping noise has remained relatively stable since its initial detection post-SM4. The overall distributions and observed negative skewness are generally consistent with the initial findings in Grogin et al. (2011), despite the σ_F and σ_G values being higher than what was originally reported: mean of $\sigma_F = 0.99e^-$ and $\sigma_G = 0.82e^-$ for this study, $\sigma_F = 0.90e^-$ and $\sigma_G = 0.75e^-$ from the previous study. This discrepancy can possibly be attributed to differences in striping noise isolation methods, superbiasers used (improved versions have been delivered since original



Figure 6: Scatter plot featuring the percent of 3σ and 4σ outliers in each year’s striping noise data, plotted in yellow and orange, respectively. The percentages are calculated based on a given year’s sample size: approximately 1,200,000 prior to 2015, and 600,000 for 2015 and after.

analysis), or Gaussian fitting techniques.

Despite some slight variations in later years, the standard deviation of the bias striping noise has remained consistent over time. With an average σ_F of $0.99e^-$, the striping noise contribution still remains less than 20% of the average WFC read noise, $\sim 4.0e^-$ from July 2009 to January 2013, $\sim 4.3e^-$ from February 2013 to June 2020, and $\sim 4.5e^-$ from July 2020 to present, which has risen due to the instability of amplifier D. The scatter in standard deviation also happens primarily at the $\pm 0.02e^-$ level, as in the previous analysis, negligible when compared to the $4.0 - 4.5e^-$ read noise contribution.

When considering the significance of the skewness and kurtosis results, we must first define the acceptable range of values for these metrics. In general, skewness and kurtosis values between -1 and $+1$ are acceptable for a normal distribution (Mishra et al., 2019). The skewness and kurtosis measurements for our data range from -0.35 to -0.27 and -0.05 to $+0.12$, respectively. Although the bias striping distributions are slightly negatively skewed and, in years 2019, 2021, and 2022, more peaked, the data are still largely consistent with a

normal distribution.

The sigma, skewness, and kurtosis results suggest that the bias striping distribution characteristics remain relatively consistent over the years, with slight deviations, particularly in 2019, 2021 and 2022. These years present with the lowest σ_F values, as well as the highest skewness and kurtosis measurements, manifesting in the form of slightly taller distributions with longer, but less negatively skewed tails. Interestingly, the σ_G values for these years remain highly consistent with the other years, likely due to the fact that the Gaussian fitter provides outlier resistant estimations.

Given the the nature of the kurtosis measure and how it is related to the presence of outliers, the observed increase in kurtosis for 2019, 2021, and 2022 would suggest a higher number of outliers in the data for these years. Because sigma clipping was applied in two different steps during the striping noise extraction, no extreme, 5σ outliers were found in any year’s data. The incidence of 4σ outliers appears to be random, while the distribution of 3σ outliers highly resembles that of the kurtosis, with clear increases in 2019, 2021, and 2022.

A greater number of 3σ outliers could certainly explain the higher kurtosis measurements for these years, and can possibly contribute to the observed differences seen in skewness and σ_F as well. The exact reason these years have an increased number of outliers is yet unknown. Since the skewness and kurtosis measurements are still within the accepted range for a normal distribution, and the σ_G values for these years remain unaffected, it may be the case that the deviations seen in 2019, 2021, and 2022 are merely sampling variations in the striping noise data.

5 Conclusion

The horizontal, low-level “bias striping” noise found in post-SM4, ACS/WFC bias frames is uniform across CCD rows, and can be effectively removed in calibration using the `acs_destripe` tool in `calacs`. The stability of this striping noise was previously studied following SM4, where it was found to be highly stable over the year period analyzed. This study expands upon the previous analysis, using raw bias frames to isolate the striping noise intensity per row in an effort to map the long-term stability of bias striping noise from 2009 through 2023.

Histograms were generated from each year’s striping noise data, and a similar, negatively skewed distribution was revealed for all years. The standard deviation of the full distribution and best-fit Gaussian model were calculated for each year, with average values of $0.99e^-$ and $0.82e^-$, respectively. With average WFC read noise values between $4.0e^-$ and $4.5e^-$ for this time period, we confirm that the striping noise contribution continues to remain less than 20% of the read noise.

Additional metrics like skewness and kurtosis were used to further study the distribution characteristics, showing that the striping noise intensity has remained relatively consistent over the years, with the exception of slight deviations seen in 2019, 2021, and 2022. Data for these years were shown to have a higher number of 3σ outliers present, likely contributing to the observed increase in skewness and kurtosis values for these years. As a result, these years feature distributions that are slightly more peaked and less negatively skewed than other years.

Despite the statistical differences observed in years 2019, 2021, and 2022, the variations were found to be within acceptable range for a normal distribution, and the standard deviation of the Gaussian model for these years remains unaffected. We therefore attribute the deviations seen in these years to sampling variations in the data. Given the overall consistency in amplitude and distribution characteristics of the bias striping noise over time, we conclude that the striping noise intensity in the ACS/WFC has remained stable over the 15 years since its initial detection in 2009.

6 Acknowledgements

The authors would like to thank the following ACS team members for their helpful comments on this report: Tri Astraatmadja, Gagandeep Anand, David Stark, Yotam Cohen, Jenna Ryon, and Amy Jones.

References

- Golimowski, D., & Ogaz, S. 2015, CCD Daily Monitor (Part 2), HST Proposal 13953
- Grogin, N. A., Lim, P. L., Maybhate, A., Hook, R. N., & Loose, M. 2011, Post-SM4 ACS/WFC Bias Striping: Characterization and Mitigation, Tech. Rep. ACS ISR 2011-05, STScI
- Koposov, S., Rivers, M., & Markwardt, C. B. 2024, Levenberg-Marquardt Fitter (MPFIT), GitHub, <https://github.com/segasai/astrolibpy/blob/master/mpfit/mpfit.py>
- Mishra, P., Pandey, C. M., Singh, U., et al. 2019, Descriptive Statistics and Normality Tests for Statistical Data, https://doi.org/10.4103/aca.ACA_157_18